Immediate Postablation ^{18}F-FDG Injection and Corresponding SUV Are Surrogate Biomarkers of Local Tumor Progression After Thermal Ablation of Colorectal Carcinoma Liver Metastases

Francois H. Cornelis[1,2], Elena N. Petre[1], Efsevia Vakiani[3], David Klimstra[3], Jeremy C. Durack[1], Mithat Gonen[4], Joseph Osborne[1], Stephen B. Solomon[1], and Constantinos T. Sofocleous[1]

[1]Interventional Radiology Service, Department of Radiology, Memorial Sloan Kettering Cancer Center, New York, New York; [2]Department of Radiology, Université Pierre et Marie Curie, Sorbonne Université, Tenon Hospital, Paris, France; [3]Department of Pathology, Memorial Sloan Kettering Cancer Center, New York, New York; and [4]Department of Epidemiology and Biostatistics, Memorial Sloan Kettering Cancer Center, New York, New York

The aim of this study was to determine whether intraprocedural ^{18}F-FDG PET/CT can be used as a predictor of local tumor progression after percutaneous ablation of colorectal liver metastases. **Methods:** In this institutional review board–approved prospective study, 39 patients (19 men and 20 women; median age, 56 y) underwent split-dose ^{18}F-FDG PET/CT-guided ablation followed by immediate biopsy and contrast-enhanced CT imaging of the ablation zone. Binary categorization of biopsy tissues was performed on the basis of the presence of only nonviable coagulation necrosis or viable tumor cells. Minimum ablation margin measurements from contrast-enhanced CT imaging were categorized as 0 mm, 1–4 mm, 5–9 mm, or greater than or equal to 10 mm. SUVs were obtained from PET/CT imaging, and SUV ratios were calculated from 3-dimensional regions of interest located in the ablation zone and surrounding normal liver. All predictive variables (biopsy, minimum margin distance, and SUV ratio) were evaluated as predictors of time to local tumor progression identified on imaging using competing-risks regression models (uni- and multivariate analyses). **Results:** A total of 62 consecutive ablations were evaluated. The mean SUV ratio was significantly higher for viable tumor–positive immediate postablation biopsies (n = 10) than for tumor-negative biopsies (n = 52) (85.8 ± 92.2 vs. 42.3 ± 45.5) (P = 0.03) and for a minimum margin size of less than 5 mm (n = 15) than for a minimum margin size of greater than or equal to 5 mm (n = 47) (78.5 ± 99.1 vs. 38.3 ± 78.5) (P = 0.01). After a median follow-up period of 22.5 (range, 7–52) months, 23 of 62 ablated tumors showed local tumor progression (37.1%). The local tumor progression rate was significantly higher for viable tumor–positive biopsies (8/10) than for negative biopsies (15/52) (80% vs. 29%) (P = 0.001) and for a minimum margin size of less than 5 mm (9/15) than for a minimum margin size of greater than or equal to 10 mm (2/15) (60% vs. 13%) (P = 0.02) but not 5–9 mm (37.5%; 12/32) (P = 0.5). In a competing-risks analysis, biopsy results (P = 0.07) and the minimum margin size (P = 0.08) were borderline significant, but the SUV ratio was not (P = 0.22). However, for negative biopsy ablations, the minimum margin size and SUV ratio were predictive imaging factors for local tumor progression; subdistribution hazard ratios were 0.564 (0.325–0.978) (P = 0.04) and 1.005 (1.001–1.009) (P = 0.005), respectively. **Conclusion:** The SUV ratio and minimum margin size can independently predict colorectal metastasis local tumor progression after liver ablation when there are no viable tumor cells on immediate postablation biopsies.

Key Words: thermal ablation; PET/CT; interventional radiology; imaging biomarkers; recurrence

J Nucl Med 2018; 59:1360–1365
DOI: 10.2967/jnumed.117.194506

A method for immediate intraprocedural treatment assessment analogous to the use of intraoperative frozen-section pathology is currently not available for percutaneous tumor ablation. Intraprocedural imaging assessment of ablation efficacy would enable additional targeted ablation if correlated with a residual viable tumor (*1*). A validated, reliable surrogate imaging biomarker of incomplete tumor ablation could be used for treatment modification without the need for biopsy.

^{18}F-FDG PET/CT is a sensitive indicator of tumor cell viability relative to anatomic imaging modalities, such as conventional CT, MRI, or ultrasound (*2,3*). Despite its relatively limited spatial resolution (*4*), PET/CT imaging has been successfully used as a reliable immediate surrogate imaging biomarker of complete ablation of ^{18}F-FDG–avid hepatic tumors, predicting 12-mo postablation local tumor control (or progression) (*1,5*). The feasibility of a split-dose ^{18}F-FDG PET/CT technique for ablation targeting of hepatic tumors as well as intraprocedural efficacy assessment has been demonstrated (*6*). A standard ^{18}F-FDG diagnostic activity dose is delivered in 2 portions, before and after ablation. The first dose decays significantly by the time the second dose is given because of the relatively short half-life of ^{18}F-FDG. Therefore, ^{18}F-FDG uptake after ablation reflects the metabolic state of the ablation zone overcoming the background signal of the initial, smaller ^{18}F-FDG dose.

The purpose of this study was to determine whether intraprocedural ^{18}F-FDG PET/CT imaging can serve as a predictor of local tumor progression after percutaneous ablation of colorectal liver metastases.

Received Oct. 30, 2017; revision accepted Jan. 3, 2018.
For correspondence or reprints contact: Constantinos T. Sofocleous, Department of Radiology, Memorial Sloan Kettering Cancer Center, 1275 York Ave., New York, NY 10065.
E-mail: sofoclec@mskcc.org
Published online Feb. 9, 2018.

MATERIALS AND METHODS

Patient Selection

This study was approved by the Institutional Review Board at Memorial Sloan Kettering Cancer Center with patient informed consent and compliance with the Health Insurance Portability and Accountability Act. Between 2011 and 2015, we prospectively enrolled patients undergoing ablation of colorectal liver metastases followed by biopsy of the ablation zone. The use of intraprocedural split-dose ^{18}F-FDG PET imaging for continuous visualization of hypermetabolic metastases was necessary for inclusion in this study (*6*). In addition, patients were eligible if they had up to 3 colorectal cancer metastases up to 3 cm in diameter and no more than 3 extrahepatic sites of disease (including lymph nodes and pulmonary nodules). We excluded patients with uncorrectable coagulopathy (international normalized ratio of >1.5 or a platelet count of <50,000/mm^3), patients who were unable to undergo general anesthesia, patients with non–^{18}F-FDG–avid colorectal liver metastases, and patients with a follow-up of shorter than 12 mo.

PET/CT-Guided Ablation

All ablations were performed by a board-certified interventional radiologist with 15 y of experience. Ablations were performed under general anesthesia in a dedicated PET/CT interventional suite (Discovery D690; GE Healthcare). The ablation modality (microwave, radiofrequency, or irreversible electroporation) was determined by the operator on the basis of several factors, including tumor size, tumor proximity to blood vessels or bile ducts, and adjacent structures. Tumors that were located less than 1 cm from a major bile duct or a major blood vessel (0.7 mm or larger in diameter) and those that were in proximity to the gastrointestinal tract and could not be protected with hydrodissection or other protective maneuvers were treated by irreversible electroporation.

An intraprocedural split-dose ^{18}F-FDG (Cardinal Health) PET imaging protocol similar to those reported previously (*5,6*) was used in all cases. In brief, each patient received an initial ^{18}F-FDG dose (mean ± SD, 159.1 ± 11.1 MBq; median, 159.1; range, 144.3–177.6) equivalent to one-third of the standard diagnostic ^{18}F-FDG dose (mean uptake time, 84.2 ± 33.6 min; median, 62; range, 45–124) and then a second ^{18}F-FDG injection (mean, 307.1 ± 33.3 MBq; median, 321.9; range, 162.8–325.6) equivalent to two-thirds of the standard diagnostic ^{18}F-FDG dose on completion of the ablation (mean uptake time, 55.6 ± 20.5 min; median, 57; range, 20–110). The patients remained on the table during the whole procedure.

In each case, localizing PET/CT was performed with ventilator-assisted breath-hold for PET acquisition (~1 min) as well as a noncontrast hepatic CT scan (~30 s). Placement of the ablation applicator was performed using conventional-mode CT, CT fluoroscopy or, occasionally, ultrasound guidance without contrast injection. Serial CT images of the applicator were obtained and fused with the initial PET dataset to confirm accurate targeting. Applicator repositioning and overlapping ablations were performed with the intention of achieving a minimum ablation margin of 5 mm around each tumor. In all cases, regardless of ablation modality, the recommended manufacturer protocol was applied and completed. At the end of ablation, in addition to PET imaging, a triple-phase contrast-enhanced CT scan was obtained to assess the ablation zone.

Immediate Postablation Biopsy Analysis

Immediately after each ablation, 2–4 image-guided biopsy samples were acquired using coaxial 18- to 20-gauge core needles as previously described (*7*). In most cases, needles were repositioned to obtain samples from the central region of the tumor and the radiographic ablation margin. For smaller tumors, a single, 2-cm-long core biopsy extended from the center to the periphery of the ablation zone.

Tissue specimens were fixed with formalin and stained with hematoxylin–eosin for morphologic assessment by a pathologist. Specimens displaying only characteristics of necrosis and no identifiable tumor cells were classified as coagulation necrosis and did not require further evaluation. Specimens containing tumor cells were further analyzed with immunohistochemical markers for proliferative potential (Ki-67), mitochondrial viability (oxidative phosphorylation antibody), and apoptosis (caspase-3 or terminal deoxynucleotidyl transferase–mediated dUTP nick-end labeling [TUNEL]). Tumor cell Ki-67 positivity, oxidative phosphorylation antibody viability, or both led to classification of the specimen as containing viable tumor cells, whereas the absence of these markers and a positive apoptotic caspase-3 or TUNEL assay led to classification of the specimen as necrosis only. In cases of mixed results (caspase-3 or TUNEL positive and tumor cells positive for Ki-67, oxidative phosphorylation antibody, or both), samples were classified as possessing viable tumor cells.

Postablation Contrast-Enhanced CT Analysis

The minimum margin size of the ablation zone was measured after ablation on contrast-enhanced CT as previously described (*8*). On a PACS workstation, the distances from the edge of the tumor to anatomic landmarks were measured on both pre- and postablation studies. For each landmark, the preablation distance was subtracted from the postablation distance to yield the margin at that site; the smallest value was considered to be the minimum margin and was recorded. Four categories of minimum margin size were considered: 0 mm, 1–4 mm, 5–9 mm, and 10 mm or larger.

Postablation ^{18}F-FDG PET/CT Quantitative Imaging Analysis

We calculated the SUV ratio for ^{18}F-FDG in the ablation zone by comparing preablation planning and postablation PET/CT images. This semiautomated method was performed independently by 2 authors by calculating the ^{18}F-FDG uptake in a rectangular 3-dimensional region of interest (ROI) including the whole ablation zone and margins (ROI-1). The ROI was measured on attenuation-corrected PET images. In addition, a 3-dimensional ROI was obtained in the noninvolved liver (ROI-2) for comparison. Assessment was performed on a dedicated workstation (TeraRecon), on which the SUV_{max} and SUV_{mean} were recorded. The SUV ratio was then calculated to normalize uptake in the ablation zone with background liver uptake as follows: SUV ratio = [(ROI-1 SUV_{max} − ROI-2 SUV_{mean})/ROI-2 SUV_{mean}] × 100.

Follow-up Clinical and Imaging Assessments

Follow-up clinical and imaging assessments on contrast-enhanced CT scans were performed at 6 wk after ablation and every 3 mo thereafter. Evidence of tumor on the 6-wk contrast-enhanced CT scan was considered ablation failure. Identification of tumor within 1 cm from the ablation zone after 6 wk was considered local tumor progression.

Statistical Analysis

Median follow-up time was calculated for patients who were alive at the end of the study period. To assess the value of the SUV ratio in addition to biopsy results and CT imaging, mean SUV ratios were calculated for the biopsy and margin size categories and comparisons were made using the Wilcoxon rank sum test. All 3 predictive variables (mean SUV ratio, biopsy result, and minimum margin size) were also evaluated for their ability to predict time to local tumor progression. For both univariate and multivariate analyses, we used competing-risks (*9*) regression models because the analyses had to account for the competing event of death.

All statistical comparisons were performed with statistical software (Stata software; StataCorp). Statistical significance was indicated by a P value of less than 0.05.

TABLE 1
Average SUVs of ROIs Before and After Ablation

ROI	SUV_{mean}	SUV_{max}
Including tumors		
Before ablation	9.2 (6.2)	2 (0.6)
After ablation	4.5 (1.7)	2.2 (0.6)
Including liver background only		
Before ablation	3.8 (1.6)	2.5 (0.5)
After ablation	4 (0.9)	3.2 (0.6)

Values in parentheses are SDs.

RESULTS

Patient Characteristics

Altogether, 94 ablations were performed in 68 patients during the study period, and 62 ablations in 39 patients met the inclusion criteria (20 women and 19 men). The median patient age was 56 y (mean, 54.6 ± 12.7; range, 32–81). Each patient had 1–3 ablated tumors (mean size, 16.8 ± 4.9 mm; median, 16; range, 6–28). Ablation modalities included microwave ($n = 46$), radiofrequency ($n = 13$), and irreversible electroporation ($n = 3$). Baseline contrast-enhanced CT and PET/CT were performed within 30 d before ablation.

The mean plasma glucose level before the first administration of ^{18}F-FDG was 116.8 ± 31.5 mg/dL (median, 106; range, 75–180). The mean time between the first and second administrations was 205 ± 34 min (median, 207; range, 82–363). SUVs are reported in Table 1.

Correlation of SUV Ratio with Biopsy and CT Findings

Table 2 shows the mean SUV ratios in relation to biopsy results and minimum margin size on CT. Biopsies of tissue specimens from ablation zones identified coagulation necrosis in 52 tumors (83.9%; 52/62) and viable tumor in 10 (16.1%; 10/62). The SUV ratio was significantly higher for positive biopsies (mean, 85.8 ± 92.2; $n = 10$) than for negative biopsies (mean, 42.3 ± 45.5; $n = 52$) ($P = 0.03$).

The minimum margin sizes on contrast-enhanced CT were 0 mm in 5 ablation zones (8.1%; 5/62), 1–4 mm in 10 (16.1%; 10/62), 5–9 mm in 32 (51.6%; 32/62), and greater than 10 mm in 15 (24.2%; 15/62). Among the 10 viable tumors revealed by biopsies, the minimum margin size was less than 5 mm in 5 (50%). The SUV ratio was also significantly higher for ablation zones with a minimum margin size of less than 5 mm (78.5 ± 99.1; $n = 15$) than for those with a minimum margin size of greater than or equal to 5 mm (38.3 ± 21.6; $n = 47$) ($P = 0.01$) (Fig. 1).

Local Tumor Progression

After a median follow-up period of 22.5 mo (range, 7–52), local progression was observed in 23 tumors (37.1%; 23/62). The local tumor progression–free survival rates at 12 and 24 mo of follow-up were 76% (95% confidence interval [CI], 62.7–85.1) and 56% (95% CI, 40.4–69.1), respectively.

Biopsy was shown to be an independent predictor of local tumor progression. Eight of 10 viable tumors classified by biopsy led to local tumor progression on imaging, whereas 15 of 52 tumors showing coagulation necrosis led to local tumor progression ($P = 0.001$).

Local tumor progression occurred in 9 of 15 tumors (60%) ablated with a minimum margin size of less than 5 mm and in 14 of 47 tumors (29.8%) with a minimum margin size of greater than or equal to 5 mm ($P = 0.19$) (Fig. 2). Compared with a minimal margin size of greater than or equal to 10 mm on CT, a minimum margin size of less than 5 mm was shown to be predictive of local tumor progression. The local tumor progression rate was significantly higher in the group with a minimal margin size of less than 5 mm (60%; 9/15) than in the group with a minimum margin size of greater than or equal to 10 mm (13.3%; 2/15) ($P = 0.02$). However, the results for a minimal margin size of less than 5 mm were not significantly different from those for a minimal margin size of 5–9 mm (37.5%: 12/32) ($P = 0.5$).

The size of the tumors in patients with local tumor progression ranged from 10 to 28 mm (median, 17) and was not significantly different from that in patients without local tumor progression (median, 16; range, 6–28) ($P = 0.92$).

A significant difference in the SUV ratio was observed between the 23 tumors with local tumor progression (71.9 ± 86.7) and the 39 tumors without local tumor progression (36 ± 18.9) ($P = 0.01$). For tumors without viable tissue on biopsies and a minimum margin size of greater than or equal to 5 mm ($n = 42$), local tumor progression occurred in 9 of 42 cases (21.4%). All were observed to have an SUV ratio of greater than or equal to 22.74.

Survival Analysis

According to the competing-risks model, analysis showed that biopsy (subdistribution hazard ratio [sHR], 2.222 [95% CI, 0.928–5.327]; $P = 0.07$) and the minimal margin size (sHR, 0.686

TABLE 2
SUV Ratios According to Biopsies and Minimal Margin Evaluations

	SUV ratio* for minimal margin size of:				
Biopsy result	0 mm	1–4 mm	5–9 mm	≥10 mm	Total
CN	65.9 ± 15.4 (3)	76.9 ± 115.2 (7)	34.1 ± 15.3 (27)	36.2 ± 21.9 (15)	42.3 ± 45.5 (52)
VTC	203.5 ± 181.0 (2)	48.0 ± 43.3 (3)	61.4 ± 35.5 (5)		85.8 ± 92.2 (10)
Total	121 ± 118.2 (5)	68.3 ± 97.3 (10)	38.4 ± 21.4 (32)	36.2 ± 21.9 (15)	

*Values are reported as mean ± SD, with values in parentheses indicating number of samples.
CN = complete necrosis; VTC = viable tumor cells.

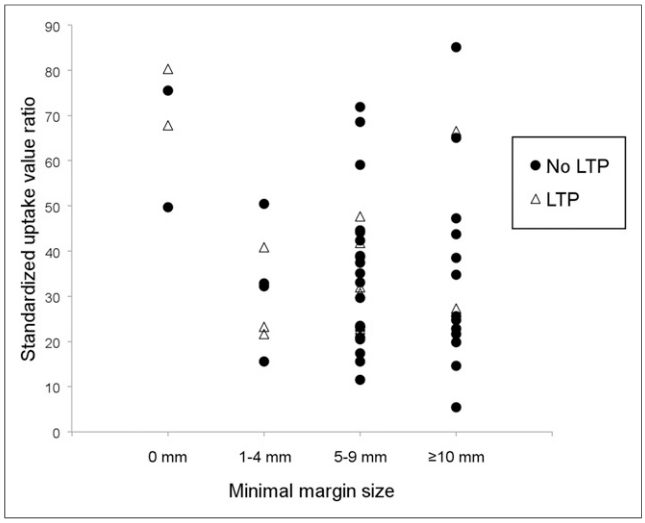

FIGURE 1. SUV ratios according to 4 groups of minimal margin size for all cases with biopsies of ablation zones that were negative for Ki-67. SUV ratios and minimal margin size were predictive of local tumor progression (LTP).

[95% CI, 0.447–1.052]; $P = 0.08$) were borderline significant predictors of local tumor progression. After multivariate analysis, the SUV ratio (sHR, 1.003 [95% CI, 0.998–1.008]; $P = 0.22$) was not significant. However, within the coagulation necrosis group ($n = 52$), multivariate analysis showed that the minimum margin size (sHR, 0.564 [95% CI, 0.325–0.978]; $P = 0.04$) and SUV ratio (sHR, 1.005 [95% CI, 1.001–1.009]; $P = 0.005$) were predictive of local tumor progression.

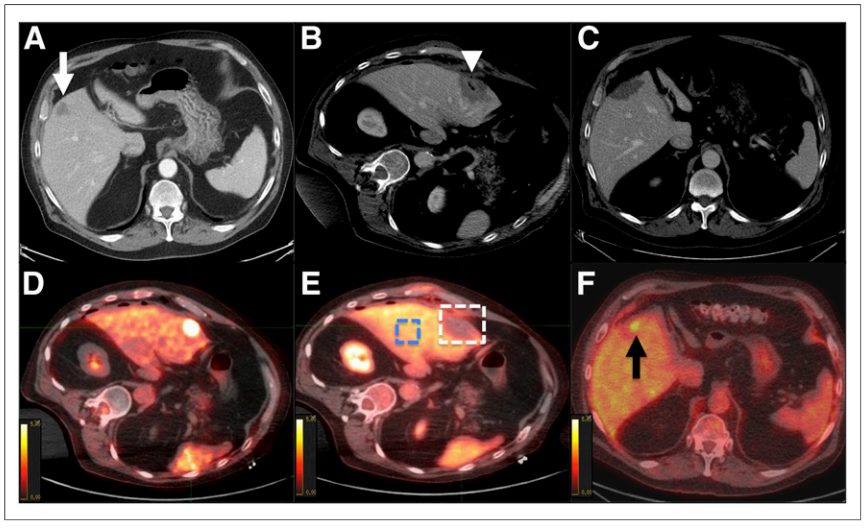

FIGURE 2. PET/CT-guided microwave ablation in 78-y-old man with 20-mm metastasis from colon adenocarcinoma. (A) Contrast-enhanced CT imaging of tumor (arrow) prior to treatment. (B) Contrast-enhanced CT imaging assessment of ablation zone (arrowhead) immediately after ablation. Minimal margin size was estimated to be 3 mm. (C) Follow-up CT scan showed no residual tumor at 6 mo. (D) Fused PET/CT imaging before ablation ($SUV_{max} = 10.6$). (E) Evaluation immediately after ablation showing equivocal residual uptake. Two 3-dimensional regions of interest were positioned on corrected PET images; 1 region included ablation zone and its margins, and 1 region included healthy liver. SUV_{mean} of liver background was 3.57, and SUV_{max} of ablation zone was 5.03. SUV ratio was 41. (F) PET/CT at 6 mo illustrating obvious uptake concordant with previous findings. Local tumor progression was identified (arrow).

DISCUSSION

In the present study, we evaluated the potential value of combining PET/CT with biopsy as a method for on-site assessment of the ablation zone to predict local tumor progression. PET/CT imaging was useful for identifying the risk of local tumor progression when biopsy samples obtained from the ablation zone did not reveal viable tumor. We also prospectively validated prior results indicating that PET/CT evaluation of the ablation zone using the split-dose technique can serve as a surrogate imaging biomarker of local tumor progression after ablation of liver metastases (*5*). The development of such intraprocedural markers of incomplete ablation could guide additional therapy, such as repeating or extending the ablation or additional treatment options (locoregional, systemic, or both). Accurate assessment of the ablation zone could decrease ablation failures by lowering the risk of local tumor progression and improving oncologic treatment efficacy (*7*).

Local tumor progression remains a significant limitation of locoregional therapies such as ablation, especially compared with metastasectomy (*8,10*). Different approaches involving imaging and pathologic assessment for detecting residual disease after ablation have been explored (*7–15*). Biopsies performed immediately after ablation with pathologic and immunohistochemical assessments of the ablation zone showed a strong correlation between identification of viable tumor cells and local tumor progression (*7*). Diffused reflectance spectroscopy was used to assess spectral changes in the ablated tissue and demonstrated that these changes correlated with the degree of thermal liver tissue damage (*16*). Our findings regarding the predictive usefulness of biopsy are in agreement with those of these previous studies. However, we were also able to demonstrate the potential of intraprocedural PET/CT imaging to improve on local tumor progression risk assessment compared with biopsy.

Previous publications revealed that biopsy evidence of complete tumor ablation and minimum ablation margins of at least 5 mm were independent predictors of local tumor control (*7,13–15,17,18*). It was also shown that for tumors ablated with radiofrequency or microwave ablation, a minimal margin of at least 10 mm was associated with no local tumor progression (*19*). Biopsy-proven tumor-negative ablation zones with margins of greater than 5 mm had sustained tumor control with local tumor progression of 3% at 30 mo after radiofrequency ablation of colorectal liver metastases (*7,8*). Although this combination is useful, biopsy results for tissue specimens from the ablation zone are typically not available until several days after the ablation, limiting the ability to modify the intraprocedural technique (*8*). Another clinical challenge is that postablation routine assessment is conducted only with imaging and without further pathologic confirmation, such as frozen-section histology (*20*). These scenarios may explain the relatively higher rates of local tumor

progression after percutaneous image-guided thermal ablation than after resection (*13–15,17,18*).

In addition to minimum margin size evaluation on CT and biopsy as proposed previously (*7,8*), PET/CT imaging provides a metabolic assessment of the ablation zone. The superiority of ^{18}F-FDG PET/CT over morphologic imaging modalities after ablation of colorectal liver metastases has been reported, with favorable sensitivity and specificity of PET/CT (92%–95% and 100%, respectively) compared with CT (83%–97% and 100%, respectively) for the detection of local tumor progression (*5*). The described method of split-dose ^{18}F-FDG PET/CT provides real-time metabolic assessment of the ablation zone, including the margins and the surrounding tissues, before any posttreatment inflammatory changes with equivocal SUV signals commence (*5,21*). In addition to ^{18}F-FDG PET/CT providing real-time metabolic assessment, prior studies also suggested that ^{18}F-FDG PET can accurately identify local recurrences as early as 3 mo after ablation (*21–23*). PET/CT within 3 mo of ablation, however, can be confounded by the presence of postablation inflammatory changes. Within a few days and for several weeks after ablation, histologic changes include a central zone of necrosis surrounded by a zone of inflammation caused by the recruitment of neutrophils, lymphocytes, and macrophages (*17,24–26*). These changes will cause increased ^{18}F-FDG uptake, which may be falsely interpreted as residual viable tumor (*27,28*). This observation justifies performing PET/CT within the initial 24 h after ablation, before the inflammatory process is evident in metabolic imaging (*5*).

The present study was limited by the relatively small numbers and a highly selected population with SUV-avid tumors. The SUV ratio was predictive of local tumor progression only in cases with coagulation necrosis. No cutoff values were obtained, as assessment of the ablation zone by biopsy was limited. The few samples that were obtained may be not representative of the whole volume of ablation. Patients whose biopsies showed viable tumor that could be targeted were retreated. Dynamic PET evaluation would allow the use of kinetic modeling instead of SUV to shorten the uptake time. As we used only 1 or 2 bed positions for PET, the frame time for PET could be increased, allowing further dose reduction. The availability of a PET/CT scanner for image-guided procedures remains low, limiting the generalization of such evaluations. However, performing ^{18}F-FDG PET/CT within 24–48 h after ablation without the need for extended anesthesia or intervention equipment may have a similar impact. This hypothesis must be evaluated in further studies. If the SUV becomes a significant surrogate for ablation and improves local control, then the development and generalization of PET/CT as a useful tool for image-guided intervention may occur.

CONCLUSION

Our method (split-dose ^{18}F-FDG PET/CT analysis) may provide an intraprocedural biomarker of local tumor progression for PET-avid colorectal carcinoma metastases in addition to biopsies and minimal margin assessments. The results of the present study illustrate that PET/CT offers additional value through the detection of partial ablation without evidence of residual viable disease by biopsy. Our study may serve as a landmark for prospective investigations to validate the initial findings and derive cutoff values. Targeting the area specific for the high SUV may help to increase the predictive value of biopsies. This feedback may allow the detection of incomplete ablation and repeat ablation while the patient is still on the procedure table. In other instances, the information can be used to encourage close follow-up for the early detection of recurrence and possible retreatment or the consideration of other therapies.

DISCLOSURE

This work was partially supported by NIH grant R21 CA131763-01A1 and through NIH/NCI Cancer Center Support grant P30 CA008748. Constantinos T. Sofocleous has received research support from Angiodynamics, Neuwave, HS Medical, and Perseon/BSD. No other potential conflict of interest relevant to this article was reported.

REFERENCES

1. Solomon SB, Cornelis F. Interventional molecular imaging. *J Nucl Med.* 2016;57:493–496.
2. McLoney ED, Isaacson AJ, Keating P. The role of PET imaging before, during, and after percutaneous hepatic and pulmonary tumor ablation. *Semin Intervent Radiol.* 2014;31:187–192.
3. Nielsen K, van Tilborg AA, Scheffer HJ, et al. PET-CT after radiofrequency ablation of colorectal liver metastases: suggestions for timing and image interpretation. *Eur J Radiol.* 2013;82:2169–2175.
4. Wahl RL, Jacene H, Kasamon Y, Lodge MA. From RECIST to PERCIST: evolving considerations for PET response criteria in solid tumors. *J Nucl Med.* 2009;50(suppl 1):122S–150S.
5. Cornelis F, Storchios V, Violari E, et al. ^{18}F-FDG PET/CT is an immediate imaging biomarker of treatment success after liver metastasis ablation. *J Nucl Med.* 2016;57:1052–1057.
6. Ryan ER, Sofocleous CT, Schoder H, et al. Split-dose technique for FDG PET/CT-guided percutaneous ablation: a method to facilitate lesion targeting and to provide immediate assessment of treatment effectiveness. *Radiology.* 2013;268:288–295.
7. Sotirchos VS, Petrovic LM, Gönen M, et al. Colorectal cancer liver metastases: biopsy of the ablation zone and margins can be used to predict oncologic outcome. *Radiology.* 2016;280:949–959.
8. Shady W, Petre EN, Gonen M, et al. Percutaneous radiofrequency ablation of colorectal cancer liver metastases: factors affecting outcomes—a 10-year experience at a single center. *Radiology.* 2016;278:601–611.
9. Fine JP, Gray RJ. A proportional hazards model for the subdistribution of a competing risk. *J Am Stat Assoc.* 1999;94:496–509.
10. Wang X, Sofocleous CT, Erinjeri JP, et al. Margin size is an independent predictor of local tumor progression after ablation of colon cancer liver metastases. *Cardiovasc Intervent Radiol.* 2013;36:166–175.
11. White RR, Avital I, Sofocleous CT, et al. Rates and patterns of recurrence for percutaneous radiofrequency ablation and open wedge resection for solitary colorectal liver metastasis. *J Gastrointest Surg.* 2007;11:256–263.
12. Wang X, Erinjeri JP, Jia X, et al. Pattern of retained contrast on immediate postprocedure computed tomography (CT) after particle embolization of liver tumors predicts subsequent treatment response. *Cardiovasc Intervent Radiol.* 2013;36:1030–1038.
13. Sofocleous CT, Garg SK, Cohen P, et al. Ki 67 is an independent predictive biomarker of cancer specific and local recurrence-free survival after lung tumor ablation. *Ann Surg Oncol.* 2013;20(suppl 3):S676–S683.
14. Sofocleous CT, Nascimento RG, Petrovic LM, et al. Histopathologic and immunohistochemical features of tissue adherent to multitined electrodes after RF ablation of liver malignancies can help predict local tumor progression: initial results. *Radiology.* 2008;249:364–374.
15. Sofocleous CT, Garg S, Petrovic LM, et al. Ki-67 is a prognostic biomarker of survival after radiofrequency ablation of liver malignancies. *Ann Surg Oncol.* 2012;19:4262–4269.
16. Tanis E, Spliethoff JW, Evers DJ, et al. Real-time in vivo assessment of radiofrequency ablation of human colorectal liver metastases using diffuse reflectance spectroscopy. *Eur J Surg Oncol.* 2016;42:251–259.
17. Sofocleous CT, Klein KM, Hubbi B, et al. Histopathologic evaluation of tissue extracted on the radiofrequency probe after ablation of liver tumors: preliminary findings. *AJR.* 2004;183:209–213.

18. Snoeren N, Huiskens J, Rijken AM, et al. Viable tumor tissue adherent to needle applicators after local ablation: a risk factor for local tumor progression. *Ann Surg Oncol.* 2011;18:3702–3710.
19. Shady W, Petre EN, Do KG, et al. Percutaneous microwave versus radiofrequency ablation of colorectal liver metastases: ablation with clear margins (A0) provides the best local tumor control. *J Vasc Interv Radiol.* 2018;29: 268–275.e1.
20. Solbiati L, Ierace T, Tonolini M, Cova L. Guidance and monitoring of radiofrequency liver tumor ablation with contrast-enhanced ultrasound. *Eur J Radiol.* 2004;51(suppl):S19–S23.
21. Vandenbroucke F, Vandemeulebroucke J, Ilsen B, et al. Predictive value of pattern classification 24 hours after radiofrequency ablation of liver metastases on CT and positron emission tomography/CT. *J Vasc Interv Radiol.* 2014;25: 1240–1249.
22. Blokhuis TJ, van der Schaaf MC, van den Tol MP, Comans EF, Manoliu RA, van der Sijp JR. Results of radio frequency ablation of primary and secondary liver tumors: long-term follow-up with computed tomography and positron emission tomography-^{18}F-deoxyfluoroglucose scanning. *Scand J Gastroenterol Suppl.* 2004;241:93–97.
23. Sahin DA, Agcaoglu O, Chretien C, Siperstein A, Berber E. The utility of PET/CT in the management of patients with colorectal liver metastases undergoing laparascopic radiofrequency thermal ablation. *Ann Surg Oncol.* 2012;19:850–855.
24. Okuma T, Matsuoka T, Okamura T, et al. ^{18}F-FDG small-animal PET for monitoring the therapeutic effect of CT-guided radiofrequency ablation on implanted VX2 lung tumors in rabbits. *J Nucl Med.* 2006;47:1351–1358.
25. Okuma T, Okamura T, Matsuoka T, et al. Fluorine-18-fluorodeoxyglucose positron emission tomography for assessment of patients with unresectable recurrent or metastatic lung cancers after CT-guided radiofrequency ablation: preliminary results. *Ann Nucl Med.* 2006;20:115–121.
26. Goldberg SN, Gazelle GS, Mueller PR. Thermal ablation therapy for focal malignancy: a unified approach to underlying principles, techniques, and diagnostic imaging guidance. *AJR.* 2000;174:323–331.
27. Donckier V, Van Laethem JL, Goldman S, et al. [F-18] fluorodeoxyglucose positron emission tomography as a tool for early recognition of incomplete tumor destruction after radiofrequency ablation for liver metastases. *J Surg Oncol.* 2003; 84:215–223.
28. Langenhoff BS, Oyen WJG, Jager GJ, et al. Efficacy of fluorine-18-deoxyglucose positron emission tomography in detecting tumor recurrence after local ablative therapy for liver metastases: a prospective study. *J Clin Oncol.* 2002;20:4453–4458.